Design Simulations of a Micropump with Multiple Actuating Mechanisms

K. Koombua and R. M. Pidaparti

Department of Mechanical Engineering
Virginia Commonwealth University
Richmond, VA 23284, USA
Email: rmpidaparti@vcu.edu

ABSTRACT

A design of a valveless micropump with two different pumping mechanisms has been investigated in this study. The micropump consists of three nozzle/diffuser elements with an actuator unit at their side wall or top wall. The actuator unit is used to create pressure difference in the pump chambers. It is this pressure difference that propels the working fluid. A computational analysis was conducted to investigate a performance characteristic of the proposed micropump. The coupling model was developed by considering a fluid-membrane interaction within the micropump. Based on the simulation results, pumping mechanism and frequency highly affected the average flow rate of the micropump. The average flow rate of the micropump increased, reached a maximum value, and decreased with a pumping frequency. The average flow rate of the top wall micropump was about 1,000,000 times higher than that of the side wall micropump.

Keywords: valveless micropump, nozzle/diffuser element, PDMS membrane, computational fluid dynamics, fluid-structure interaction

1 INTRODUCTION

Microfluidic system is of interest in many applications, e.g., drug delivery systems [1, 2], artificial prostheses [3], liquid cooling systems [4], fuel cells [5], and macromolecule and cell analysis [6] because of small volume and fast reaction time. A primary component of any microfluidic system is a micropump. A micropump is used to control a movement of a small fluid volume around a microfluidic system.

The first attempt in designing the mechanical micropump is the check-valve micropump, which consists of two check-valves and one pump chamber with an actuator unit [7]. However, there are some problems with this check-valve micropump. The flexible valve must be designed by material with a small Young's modulus to minimize the critical pressure at which the valves start opening [7]. In addition, there is a risk of valve blockage from small particles as well as wear and fatigue from moving parts [8]. The valveless micropump overcomes the disadvantages of the check-valve micropump by replacing two check valves with two nozzle/diffuser elements or valvular conduit structures. Rectification behavior of the nozzle/diffuser elements or valvular conduit structures controls fluid flow in one direction. However, there is one main drawback of the valveless micropump. Any overpressure at the outlet can cause a back flow to occur throughout the operating cycle [8]. This reverse flow decreases the average flow rate from the micropump and leads to an increase in energy consumption.

Understanding how a valveless micropump operates would help us better develop a new valveless micropump. A computational model can be used as a useful aid to provide us important information about a new design of the valveless micropump. Flow inside the valveless micropump involves many physical fields; e.g. electric, solid, and fluid. The computational model incorporating all related physics give us more accurate results of the valveless micropump; however, this computational model becomes very difficult or formidable to obtain an analytical solution. With an advent of a powerful computer, a numerical analysis is chosen to obtain an approximate solution for the valveless micropump. The electric-solid-fluid coupling model of the valveless micropump has been used extensively by many researchers as a tool to investigate a parameter affecting a performance characteristic of the valveless micropump [9, 10]. In this paper, the coupling model was used to analyze a performance characteristic of a proposed valveless micropump. The simulation results will be used to determine the optimum pumping mechanism and frequency of the micropump prototype developed at Virginia Commonwealth University.

2 DESIGN OF MICROPUMP

The designed polydimethylsiloxane (PDMS) micropump consists of three nozzle/diffuser elements with an actuator unit that is used to create pressure difference in the pump chamber. Pump chamber has an hourglass shape and is made of PDMS polymer. An actuator unit is a pneumatic pump chamber or a piezoelectric material. The movement of the actuator unit can be accurately controlled by an external supplied voltage. The two designs of the micropump are shown in Fig. 1. The geometry of the pump chamber for both designs is similar (1 cm x 2 cm x 50 μm); however, actuating mechanism is different. In the first design, the actuator unit, a pneumatic pump chamber, is attached to the sidewall of the pump chamber and it moves

horizontally (see Fig. 1a). For the second design, the actuator unit is a circular piezoelectric material and is attached to the top of the pump chamber. This actuator unit moves vertically (see Fig. 1b).

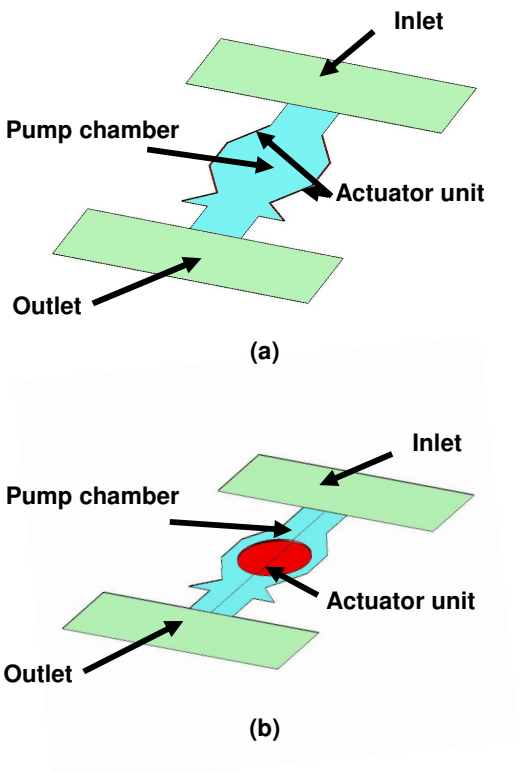

Figure 1: Two designs of the PDMS valveless micropump.

3 COMPUTATIONAL MODEL

We used the computational model to help us understand how the micropump works. The information from the computational model is used to determine appropriate pumping mechanism and frequency to achieve an optimum flow rate of the micropump. Flow within the micropump during the operation was investigated by solving two coupled sets of the governing equations with associated boundary conditions.

3.1 Governing Equations for PDMS Membranes

The governing equations for movement of the membranes during operating cycle are the time-dependent structural equations and are described below using Einstein's repeated index convention [11].

Equation of motion

$$\frac{\partial \sigma_{ij}}{\partial x_j} + F_i = \rho \frac{\partial^2 u_i}{\partial t^2} \tag{1}$$

Constitutive relations

$$\sigma_{ij} = C_{ijkl} \varepsilon_{kl} \tag{2}$$

In the equation above, σ is the stress in each direction, F is the body force, ρ is density, and u is the displacement, C is the elasticity tensor, and ε is the strain in each direction.

3.2 Governing Equations for Fluid Flow

The governing equations for transient flow within the micropump are Navier-Stokes equations on a moving mesh with the assumption of incompressible flow. These equations govern the principles of mass and momentum conservation and are described below using Einstein's repeated index convention [12].

Conservation of mass

$$\frac{\rho_g}{\sqrt{g}} \frac{\partial}{\partial t}\left(\sqrt{g}\right) + \rho_g \frac{\partial}{\partial x_j}\left(u_j - \frac{\partial \tilde{x}_j}{\partial t}\right) = 0 \tag{3}$$

Conservation of momentum

$$\frac{\rho_g}{\sqrt{g}} \frac{\partial}{\partial t}\left(\sqrt{g}\, u_i\right) + \rho_g \frac{\partial}{\partial x_j}\left[\left(u_j - \frac{\partial \tilde{x}_j}{\partial t}\right) u_i\right] = -\frac{\partial p}{\partial x_i} + \mu \frac{\partial^2 u_i}{\partial x_j^2} \tag{4}$$

In these equations, $\tilde{x}_i$ represents the moving mesh location, $\sqrt{g}$ is the metric tensor determinate of the transformation, i.e., the local computational control-volume size, ρ_g is fluid density, p is fluid pressure, μ is fluid viscosity, and u is fluid velocity.

3.3 Numerical Technique

The computational model of the micropump was created using two commercial software ANSYS [13] and ANSYS CFX [14]. ANSYS is general-purpose finite element (FE) software for structural modeling and ANSYS CFX is general-purpose computational fluid dynamics (CFD) software for modeling fluid flows. The solid domain for the computational model was the PDMS membranes and the fluid domain was fluid inside the micropump. The fluid-structure interaction (FSI) algorithm was chosen to model flow inside the micropump.

3.4 Boundary Conditions

The working fluid of the micropump was assumed to be water with density of 998.2 kg/m3 and viscosity of 0.001003 kg/m-s. The PDMS membranes were assumed to be homogeneous and isotropic material with Young's modulus of 750 kPa, density of 965 kg/m^3, and Poisson's ratio of 0.49. Pressure levels at both inlet and outlet were constant pressure at 0 Pa. These boundary conditions represent a pressure head of 0 Pa. The no-slip boundary

condition was applied at an interface between PDMS membranes and working fluid.

3.5 Method of Analysis

The time step for each pumping frequency was determined such that for one operating cycle, 100 time steps were used. The following equation was used to evaluate the time step for each case.

$$\Delta t = \frac{1}{100\, f} \tag{5}$$

The average flow rate at the specific pumping frequency f was carried on when the transient response of the flow rate at the outlet of the micropump reached a steady state. The following equation was used to calculate the average flow rate.

$$\dot{q}_{mean} = \frac{1}{T}\int_0^T q(t)\, dt \tag{6}$$

where T is the period for one operating cycle (s) and $q(t)$ is the transient response of the flow rate at the outlet of the micropump (m^3/s).

To simulate the movement of the PDMS membranes for the side wall pumping mechanism, the 1-Pa pressure was applied on the side wall of the micropump with a specific sequence; two consecutive membranes decreased the pump chambers while other two membranes increased the pump chambers. In contrast, the voltage of 10 V was applied at the piezoelectric material for the top wall pumping mechanism. In supply mode, the piezoelectric material pulled the PDMS membrane up generating a low pressure in the chamber and the piezoelectric material pushed the PDMS membrane down generating a high pressure in the chamber during pumping mode.

4 RESULTS AND DISSCUSSION

Simulations were conducted to investigate the influence of pumping mechanism, and pumping frequency on the average flow rate of the micropump. Since fluid velocity and pressure within the micropump were similar for all pumping frequencies and pumping mechanisms. The results for the micropump operating at 0.5 Hz for the top wall pumping mechanism are shown here. During the supply mode, pressure in the pump chamber near the inlet was lower than pressure in the inlet reservoir and pressure within the micropump were higher than that at the outlet reservoir. This caused fluid to move from the inlet reservoir into the micropump and eventually went through the outlet reservoir (see Figure 2). The high pressure within the micropump also prevented a backflow from the outlet reservoir into the micropump. During the pumping mode, pressure in the pump chamber near the outlet reservoir was the lowest and its pressure was greater than that in the outlet reservoir. This caused fluid to move from the micropump into the outlet reservoir (see Figure 3). The maximum fluid velocity during the supply mode, 4.72E-11 m/s, was higher than that during the pumping mode, 5.97E-12 m/s.

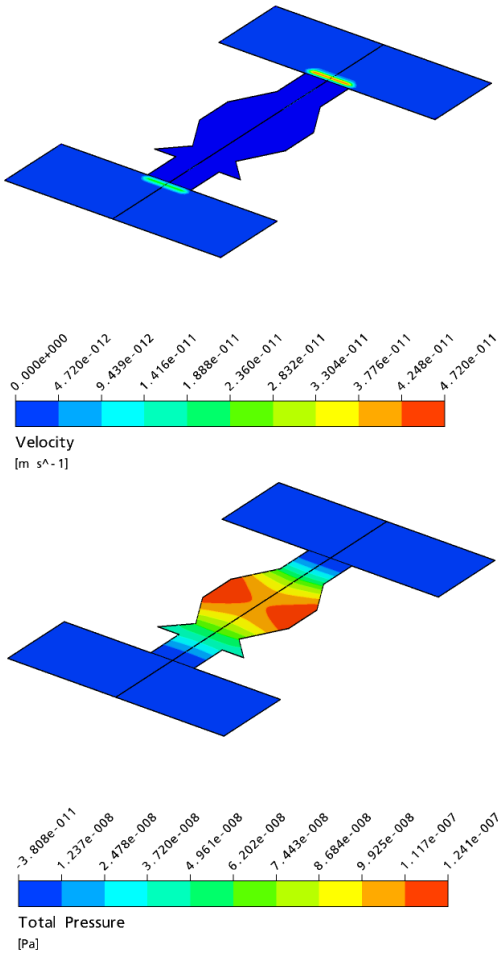

Figure 2: Fluid velocity (top) and pressure (bottom) during the supply mode of the micropump operating at 0.5 Hz in the side wall pumping mechanism.

Although the fluid pressures during the operation of the micropump in the top wall pumping mechanism were similar to those of the side wall pumping mechanism, the maximum fluid velocity for the micropump operating in the top wall pumping mechanism was much higher than that in the side wall operating mode. The maximum fluid velocity for the supply mode was 1.31E-4 m/s and the maximum fluid velocity for the pumping mode was 1.30E-4 m/s.

The average flow rate of the micropump operating at various frequencies is shown in Figure 4. As can be seen from this figure, the average flow rate varied non-linearly with the frequency. The average flow rate increased with an increasing frequency until 0.5 Hz. Then, the average flow rate started decreasing when the frequency was higher than

0.5 Hz. The possible reason for the decrease flow rate is water has its own momentum. At a high frequency, water cannot vibrate synchronously with the PDMS membrane. This caused a decrease in the average flow rate at the outlet of the micropump. The maximum average flow rates were 2.09e-11 and 3.40e-03 µl/min for side wall and top wall pumping mechanism, respectively. These results suggest that the micropump should be operated at pumping frequency of 50 Hz in both pumping mechanisms to obtain the optimum flow rate.

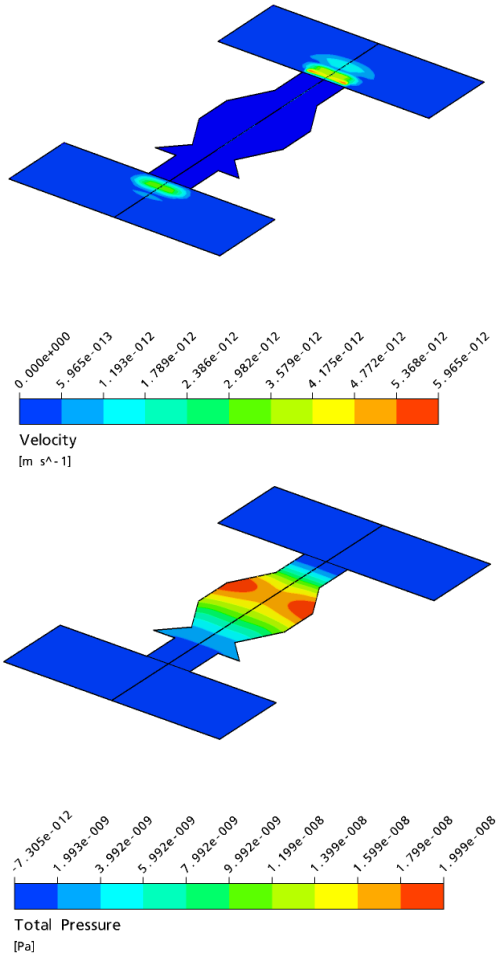

Figure 3: Fluid velocity (top) and pressure (bottom) during the pumping mode of the micropump operating at 0.5 Hz in the side wall pumping mechanism.

Comparing the average flow rate between two pumping mechanisms at the same frequency and power input, we found that the top wall pumping mechanism can provide more average flow rate than side wall pumping mechanism about 1,000,000 times. These simulation results will be used to guide an experiment of the micropump prototype that is fabricated in our clean room.

ACKNOWLEDGMENT

The authors thank the US National Science Foundation for sponsoring the research reported in this study through a grant ECCS-0725496.

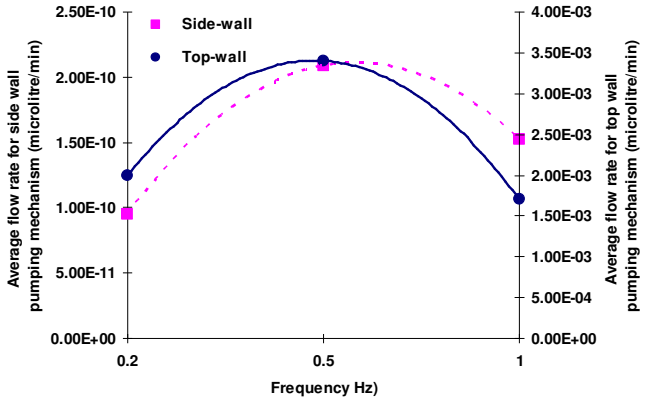

Figure 4: The average flow rate of the micropump operating in the side wall and top wall pumping mechanisms at various frequencies.

REFERENCES

[1] L. Cao, S. Mantell, and D. Polla, Sensors and Actuators A, 94, 117-125, 2001

[2] K. Junwu, Y. Zhigang, P. Taijiang, C. Guangming C, and W. Boda W, Sensors and Actuators A, 121, 156-161, 2005

[3] A. Doll, M. Heinrichs, F. Goldschmidtboeing, H. J. Schrag, U. T. Hopt, and P. Woias, Sensors and Actuators A, 130-131, 445-453, 2006

[4] V. Singhal, S. V. Garimella, IEEE Transactions on Advanced Packaging, 28, 216-230, 2005

[5] T. Zhang and Q. Wang, Journal of Power Sources, 140, 72-80, 2005

[6] D. J. Beebe, G. A. Mensing, and G. M. Walker, Annual Reviews of Biomedical Engineering, 4, 261-286, 2002

[7] N. Nguyen, X. Huang, and T. K. Chuan, Journal of Fluids Engineering, 124, 384-392, 2002

[8] P. Woias, Sensors and Actuators B, 105, 28-38, 2005

[9] Q. Cui, C. Liu, X. F. Zha, Microfluidic and Nanofluidic, 3, 377-390, 2007

[10] Q. Yao, D. Xu, L. S. Pan, A. L. M. Teo, W. M. Ho, V. S. P. Lee, and M. Shabbir, Engineering Application of Computational Fluid Mechanics, 1, 181-188, 2007

[11] J. N. Reddy, "An Introduction to the Finite Element Method", McGraw-Hill, New York, NY, 1993

[12] P. W. Longest, C. Kleinstreuer, Aerosol Science and Technology, 39, 124-138, 2005

[13] ANSYS, "ANSYS 11.0 User Guide", ANSYS Inc., Canonsburg, PA, 2007

[14] ANSYS, "ANSYS CFX 11.0 User Guide", ANSYS Inc., Canonsburg, PA, 2007